Paleomagnetic directions from mid-latitude sites in the southern hemisphere (Argentina): Contribution to Time Averaged Field models

X. Quidelleur, J. Carlut, P. Tchilinguirian, A. Germa, P.-Y. Gillot

Accepted Manuscript

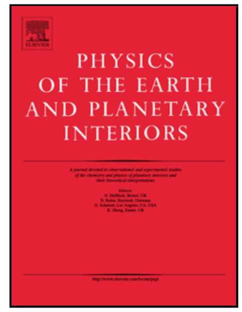

Title: Paleomagnetic directions from mid-latitude sites in the southern hemisphere (Argentina): Contribution to Time Averaged Field models

Authors: X. Quidelleur, J. Carlut, P. Tchilinguirian, A. Germa, P.-Y. Gillot

PII: S0031-9201(08)00247-1
DOI: doi:10.1016/j.pepi.2008.09.012
Reference: PEPI 5066

To appear in: *Physics of the Earth and Planetary Interiors*

Received date: 20-5-2008
Revised date: 2-9-2008
Accepted date: 10-9-2008

Please cite this article as: Quidelleur, X., Carlut, J., Tchilinguirian, P., Germa, A., Gillot, P.-Y., Paleomagnetic directions from mid-latitude sites in the southern hemisphere (Argentina): Contribution to Time Averaged Field models, *Physics of the Earth and Planetary Interiors* (2008), doi:10.1016/j.pepi.2008.09.012

Paleomagnetic directions from mid-latitude sites in the southern hemisphere (Argentina): Contribution to Time Averaged Field models

Quidelleur, X.[1,*], Carlut, J.[2], Tchilinguirian P.[3], Germa, A.[1] and Gillot, P.-Y.[1]

[1] Laboratoire de Géochronologie, UMR IDES 8148, Université Paris-Sud 11, Orsay, France.

[2] Laboratoire de Geologie, UMR 8538, Ecole Normale Supérieure, Paris, France.

[3] SEGEMAR, Universidad de Buenos Aires, Buenos Aires, Argentina.

[*] Corresponding author: xavier.quidelleur@u-psud.fr

PEPI-D-08-00112; ***Revised version (Sept. 2008)***

Abstract

Back-arc volcanism located to the east of the Andean Cordillera was sampled in the Argentina provinces of Mendoza and Neuquen for paleomagnetic time average field and paleosecular investigations. The activity ranges from 2 Ma to very recent time, with a large variety of products, from basalts to highly differentiated lavas. After removal of sites affected by lightning, those with α_{95} higher than 10°, and combining of nearby sites displaying close directions, we present new paleomagnetic results from 31 flows units belonging to two volcanic massifs: the Payun Matru and the Cerro Nevado. Previous and new K-Ar age determinations constrain the volcanic activity of these massifs from 300 to 0 ka, and from 1.9 to 0.9 Ma, respectively. Most paleomagnetic samples have NRM intensities between about 1 and 20 A/m and depict progressive removal of magnetization components in a consistent fashion during stepwise AF or thermal demagnetization. Nineteen flows yielded a normal direction (declination = 354.8°, inclination = -53.0°, α_{95} = 6.8°) and 12 flows a reverse direction (declination = 181.0°, inclination = 52.3°, α_{95} = 5.9°). The combined data yielded a mean direction (declination = 357.3°, inclination = -52.8°, α_{95} = 4.6°), which is not statistically different from the axial dipole field (g_1^0) expected at this latitude (36°S). The angular dispersion of virtual geomagnetic poles calculated from flows with normal directions (ASD = 16.5°) compares well with the observed value from global datasets for this site latitude, but flows with reverse directions display a surprisingly low dispersion (ASD = 12.5°). Since most reverse directions were sampled from flows ranging between 1.9 and 0.9 Ma, this can be interpreted as an interval of low paleomagnetic secular variation. Additional data, also with accurate time constraints, are obviously needed to better support this observation. Finally, no convincing evidence for a complex time average field significantly different from the axial dipole can be supported by this study for the last 2 Myr.

Keywords: Time averaged field; Paleosecular variation; paleomagnetism; K-Ar dating; Back-arc volcanism; Argentina

1. Introduction

When averaged over a large time interval the Earth magnetic field, or time average field (TAF), is similar to that of a geocentric axial dipole (GAD). Such assumption allows the calculation of the paleolatitude (λ) as a simple function of the paleomagnetic inclination (I) recorded in rocks, through the formula: tan (I) = 2 tan (λ). It has been widely used for plate tectonics reconstructions, and such simple geometry of the TAF has strong implication for our knowledge of the geodynamo. Although it is generally accepted to a first order, early global paleomagnetic studies (Wilson, 1971) have evidenced a significant departure from this simple model, best accounted for an offset axial dipole, i.e., by the presence of a persistent axial quadrupole superimposed to the GAD.

More recently, various attempts have been made to detect any persistent departure from the GAD model, with two main kinds of TAF models proposed. The first kind (e.g., Merrill and McFadden, 2003; Quidelleur et al., 1994; Schneider and Kent, 1990) displays a zonal geometry with various contributions of persistent axial quadrupolar (g_2^0) and/or octupolar (g_3^0) terms. More complicated models based on inverse calculations have suggested much complex geometries, with persistent features of higher degree and order (e.g., Gubbins and Kelly, 1993; Johnson and Constable, 1997). However their robustness has been questioned (Carlut and Courtillot, 1998), mostly on the basis of the poor geographic distribution of sampling sites incorporated in paleomagnetic datasets covering the last 5 Myr (Johnson and Constable, 1995; McElhinny and McFadden, 1997;

Quidelleur et al., 1994). Different approaches including the analysis of the statistical distribution of directions led to inconclusive results regarding persistent non-zonal components, thereby reinforcing simple zonal geometry models (Khokhlov et al., 2001, 2006; Tauxe, 2005).

The paleosecular variation (PSV) of the paleomagnetic field can also impact on persistent components of TAF models, depending on the geographic site distribution (Hatakeyama and Kono, 2002; Quidelleur and Courtillot, 1996). Most commonly, PSV is investigated by scrutinizing the angular standard dispersion (ASD) of virtual paleomagnetic poles (VGP) and its dependency with sampling site latitude. A pronounced increase of ASD with latitude, which has long been observed (e.g., McFadden et al., 1988), is the most striking feature. Most models proposed for PSV structure requires a non-uniform structure of the spherical harmonic coefficients in order to account for this latitudinal dependency. In these models the field model coefficients can vary as random values with a Gaussian distribution, this produces a set of field directions in each given site. Not only the mean (usually set to zero) but also the variance of the spherical harmonic coefficients allow to change the shapes of the resultant PSV distribution. This approach originally initiated by Constable and Parker (1988) provides coherent and interesting results albeit hard to directly connect to dynamo modeling. For instance, when the standard deviation of the quadrupole with spherical harmonic degree $n = 2$ and order $m = 1$ is larger than that of quadrupole terms with order $n = 0$ and $m = 2$, a best fit of the model to the paleomagnetic database is observed (Constable and Johnson, 1999; Kono and Tanaka, 1995; Quidelleur and Courtillot, 1996; Tauxe and Kent, 2004). However, such structure of the PSV might also be biased by the relatively poor geographical distribution of sampling sites. Moreover, an improved timing control of the presently available databases could allow detecting any temporal dependency of PSV, as observed for low latitude sites during the Brunhes chron (Lawrence et al., 2006).

A major effort in collecting volcanic data, which recorded accurate snapshot of the paleomagnetic field as they cooled through the Curie temperature of ferromagnetic minerals such as magnetite (about 580°C), in areas previously devoted, was since conducted. Sampling sites located in a low latitudinal band (e.g., Carlut et al., 2000; Elmaleh et al., 2004; Mejia et al., 2005; Yamamoto et al., 2002), where the inclination anomaly due to a persistent axial quadrupole superimposed to the axial dipole would be maximum, were preferentially chosen. Areas from the whole southern hemisphere were also investigated (Opdyke et al., 2006), including very high latitude sites (Baraldo et al., 2003; Tauxe et al., 2004a).

Even recently, the whole South America continent was fully lacking reliable data obtained with modern paleomagnetic techniques. Recent studies provided data from southern Patagonia (Brown et al., 2004; Mejia et al., 2004) and from the Ecuador (Opdyke et al., 2006) to fill a major geographic gap of paleomagnetic databases. In order to further improve the geographic coverage, we present here new paleomagnetic data from northern Patagonia of Argentina in the Andean Southern Volcanic Zone (SVZ). They have been obtained from more than 30 independent sites from the last 2 Myr.

2. Geological setting

The SVZ, which extents between 46 and 34°S is characterized by an active magmatic arc overlying the 30° dip eastward subduction of the Nazca plate under the South American plate. North of 34°S, the lack of active volcanism has been related to the flattening of the subduction dip (e.g., Ramos, 1999). In addition to the North South volcanic lineament of the SVZ arc, an important back-arc volcanism is observed between 36 and 38°S, north to the Mesozoic Neuquen basin. Such volcanism has been related to the change of subduction dip from Miocene to present. Kay et al. (2006) suggested that the Miocene arc-like lavas of the Sierra de Chachauén, located about 500 km east of the present-day arc, were erupted during a transient shallowing of the Andean subduction zone. Since 5 Ma, following this episode, the subduction angle steepened. The widespread back-arc volcanism of the Llancanelo Volcanic field (LLVF) and the Payun Matru Volcanic field (PMVF), with characteristic within plate signatures, has been related to the injection of hot asthenosphere into the thicker mantle wedge above the steepening slab (Kay et al., 2004).

Such magmatism is dominated by effusive volcanism, although major episode of caldera forming explosion did occur, as attested by the existence of the 7 km wide Payun Matru caldera. Basalts and basaltic andesites are dominant but highly differentiated products have been emitted as both large area ignimbrites related to caldera formation, pumice fall deposits or thick lava flows emitted along the caldera margin faults (Germa et al., 2008).

In the studied area, contractionnal regime climaxed during late Miocene in the foreland area, and was followed by Pliocene extension, which favored the eruption of the back-arc volcanism (Ramos and Kay, 2006). East of the Las Loicas trough (Figure 1), the termination of which is marked by the Tromen volcano (Folguera et al., 2006), no major post-volcanism tectonic faults have been reported. Therefore, the choice of Quaternary, far-East lying back-arc volcanism for the paleosecular variation investigation conducted here is well supported. Two main back-arc volcanic massifs have been sampled for the present study, the PMVF and the LLVF.

The PMVF is characterized by a large variety of emitted products with a very good timing constraint (Germa et al., 2008). Los Volcanes is a basaltic field with mainly effusive activity with ages covering the last 230 kyr. The occurrence of several strikingly dark flows in the satellite photo (Figure 1) strongly argues for their emplacement during the Holocene. The Payun stratovolcano has a restricted period of activity between 285 and 261 ka. The Payun Matru composite volcano lies to the north of Payun volcano and to the east of the Los Volcanes field. Its activity is constrained between 168 ± 3 ka and 7±1 ka, from ages obtained for the outer rim and for the younger intra-caldera lava, respectively. Finally, basaltic lavas from this volcanic complex can be extremely long, with length reaching 180 km (Pasquaré et al., 2008).

The Cerro Nevado volcano (3810 m) is the only major edifice of the LLVF and is dominated by trachyandesite products. Satellite photo examination shows that no recent lavas have likely erupted in its vicinity. Furthermore, erosional features such as dissected flanks and radial valleys development suggest that a relatively long time interval occurred since its last activity. Prior to the present study, no age data was available for the LLVF but it was considered to be Pliocene (Bermudez et al., 1993).

3. Techniques

3.1 Paleomagnetism

Paleomagnetic samples were collected during two field trips in December 2002 and 2003. A portable hand drill was used and orientation was made using a magnetic and a sun compass. Site locations shown in Figure 1 were determined using a GPS. A total of 49 flow units were collected during the two field trips for PMVF and LLVF areas. Twenty-three flows are from the Cerro Nevado massif (labeled CN) and 26 flows are from the Payun Matru massif (labeled PY or PN). Between 8 and 10 cores were collected from each flow.

The measurements were made in the Institut de Physique du Globe de Paris (IPGP) magnetically shielded room using a JR5 spinner magnetometer. JR5 was preferred to 2G cryogenic magnetometer because of the high magnetization of the samples. For each flow, samples were demagnetized using both thermal (20% of the samples) and alternating field (AF) demagnetization (80%). AF demagnetization was shown to be more efficient mostly because many sites were affected by lightning and were better magnetically cleaned using alternating field. Two flows (PN21 and PN27), which yielded too high magnetization intensities caused by lightning strikes (from 10 to 10^3 A/m), were discarded. The characteristic directions of magnetization were determined with the Paleomac software (Cogné, 2003), using Zijderveld projections (Zijderveld, 1967) and principal component analysis (Kirschvink, 1980), combined with great circles analysis for a few cases when the primary direction seems to be partly overlapped by a secondary component.

3.2 K-Ar dating

K-Ar dating has been performed in the present study in order to provide the first radiochronological constraints for the LLVF and to constrain the onset of volcanism in the PMVF.

Hand size samples (1-2 kg) of representative units were crushed to a 250 - 400 μm size fraction and were ultrasonically cleaned for 15 minutes in a 5% nitric acid solution to remove possible trace of weathered material. In order to make the contribution of magmatic argon and weathered phases negligible, we have removed mafic phenocrysts using heavy liquids, and analyzed only the remaining groundmass obtained within a narrow density range, typically between 2.95 and 3.00 g/cm^3. Potassium was measured by flame emission spectroscopy and was compared with reference values of MDO-G and ISH-G standards (Gillot et al., 1992). Between 1 and 2 g of sample were wrapped in Cu foil and fused for 15 minutes at temperature above 1500 °C using a high-frequency furnace, which is sufficient for complete extraction of argon from basaltic groundmass. Before analysis, multiple steps gas cleaning was performed using Ti foam at 700 °C and SAES MP-10 getters at 400 °C. Argon, the remaining gas, was measured using the K-Ar Cassignol-Gillot technique (Cassignol and Gillot, 1982), which is based on an atmospheric argon comparison, with a mass spectrometer identical to the one described by Gillot and Cornette (1986). The interlaboratory standard GL-O, with the recommended value of 6.679×10^{14} atom/g of $^{40}Ar^*$ (Odin et al., 1982), was used for ^{40}Ar signal calibration. Typical uncertainties of 1% are achieved for the ^{40}Ar signal calibration (including GL-O standard uncertainty) and for the K determination. The uncertainty on the $^{40}Ar^*$ determination is a function of the radiogenic content of the sample. The detection limit of the system is presently of 0.1% of ^{40}Ar (Quidelleur et al., 2001). All uncertainties are quoted at the 1 sigma level. The decay constants and isotopic ratios for K of Steiger and Jäger (1977) have been used throughout.

4. Results

4.1 Paleomagnetism

Examples of typical demagnetization diagrams are shown in Figure 2. All samples have lost more than 90% of their initial magnetization at 585°C or 100mT, during thermal or AF treatment, respectively, suggesting that magnetite or low Ti titanomagnetite is the main carrier of the natural remanent magnetization (NRM).

The individual characteristic direction from each sample was in most cases easily identified from both thermal and AF demagnetization techniques (Figure 2a and b). As previously recognized, AF was more efficient than thermal treatment to remove isothermal remanent magnetization (IRM) acquired during lightning strikes which was a frequently occurring feature, as illustrated in Figures 2c and d, and, 2e and f, for reverse and normal characteristic remanent magnetization (ChRM), respectively. The IRM overprint was easily removed before 10 mT, while the great circles method (Halls, 1976) was necessary to isolate the ChRM from the IRM component. The paleomagnetic direction from each flow was obtained using Fisher statistic (Fisher, 1953) or mixed statistic when great circles were necessary. Finally, a paleomagnetic direction was calculated from 40 out of the 44 units collected (Table 1). Very high scatters leading to unresolved directions and therefore rejection were most likely due to lightning, as attested by very high magnetization of some cores, or small bloc rotations unrecognized in the field. Results from the 40 flows are reported in Table 1 and in Figure 3.

A few flows that are geographically close display undistinguishable directions at the 95% level, which we interpret as the result of eruptions taking place in a narrow time-span. This is the case for CN08 and CN09, CN37 and CN38, CN40 and CN42, PY15 and PY16, and, PY21 and PY22 (shown in grey in Figure 3). In order to avoid any bias due to over-sampling, all samples have been combined before the calculation of a single mean direction for each of these couples of flows (Table 1).

From the remaining 35 mean directions, all PMVF sites (21 data) display a normal polarity, except PY21-22, and, all LLVF sites (14 data) with the exception of CN11 and CN34 are of reverse polarity. Four sites

(CN34, CN39, PY18 and PY31) yield a mean direction associated with an α_{95} above 10°, which is generally considered as an upper threshold for PSV studies. These sites will be rejected from further mean field calculations which therefore rely on 31 directions (Figure 4).

The overall mean direction calculated from the 31 sites of this study, all transformed into normal polarity, is Dec=357.3°, Inc=-52.8°, α_{95} =4.6°. The mean direction from normal (reverse) polarity flows is Dec=354.8°, Inc=-53.0°, α_{95} =6.8°, N= 19 (Dec=181.0°, Inc=52.3°, α_{95} =5.9°, N=12).

4.2 K-Ar dating

New K-Ar Cassignol-Gillot ages are given in Table 2a and b, for the LLVF and PMVF, respectively. They range from 1.88 ± 0.03 to 0.944 ± 0.016 Ma. All analyses have been duplicated and yield in all cases reproducible values at the one-sigma level. Previous ages from the PMVF (Germa et al., 2008), obtained using the same technique, for flows also sampled for the present paleomagnetic study are given in Table 3.

The ages obtained here for the LLVF provide the first radiometric dating of this extinct field. Its activity probably initiated at about 2 Ma and lasted about 1 Myr. The construction of the Cerro Nevado volcano is well constrained at 1.32 ± 0.02 Ma from two undistinguishable ages obtained for two flows (CN 11 and CN17; Table 2a) sampled at the base and towards its summit, respectively. The oldest flow dated here (CN34; 1.878 ± 0.028 Ma) is located to the south of the LLVF, while the youngest (CN42; 0.944 ± 0.016 Ma) belong to a northern volcanic center (Figure 1). Regarding PMVF, the single new age (1.72 ± 0.02 Ma, Table 2b), obtained from the northern part, is much older than the ages ranging from present to about 0.3 Ma previously reported for this volcanic field (Germa et al., 2008). Hence, it is rather recognized as from a distinct older volcanic center.

5. Discussion

5.1 Age reliability and comparison with the geomagnetic polarity time scale

Figure 5 shows the perfect agreement between the available paleomagnetic polarity (Table 1) and K-Ar ages (Table 2a and b), compared with the geomagnetic polarity time scale (GPTS; Cande and Kent, 1995). Every sites from the PMVF but PY21-22 display normal directions, in agreement with their age younger than 300 ka (Germa et al., 2008), and hence falling within the Brunhes chron. Flow PY21 dated here at 1.716 ± 0.025 Ma (Table 2b) belongs to the early Matuyama chron, as expected from its reverse polarity (Table1). Flows from the LLVF encompass four polarity changes within the Matuyama chron, from the Olduvai to the Jaramillo subchrons (Figure 5).

5.2 Mean directions

The present day field (PDF) throughout South America displays directions strongly departing from a purely dipolar field with an inclination of –35.5°, much shallower than the expected value of –55.0° from the GAD hypothesis at the present site location. Only 3 out of 31 paleo-inclinations measured in the present study (Table 1) reach the PDF value, which highlights the rather anomalous character of the latter.

As reported in Table 4 and shown in Figure 4, the mean declination for all sites, as well as for each subgroup, is undistinguishable from 0 or 180° within the α_{95} confidence cone. This shows that possible regional tectonic rotation is not a concern here, and moreover, that the paleomagnetic field at the site location is fully compatible with a zonal geometry. When comparing the inclination values and the GAD value (-55.0°), all subgroups from Table 4 display a slightly shallower direction, although it also remains within the α_{95} confidence cone. There is no difference between normal and reverse, nor between the two time intervals investigated here. The time dependency of the TAF suggested in some earlier studies at the 10^4 to 10^5 years timescale (Carlut et al., 2000; Elmaleh et al., 2004; Zanella, 1998) does not seem to be observed here at the 10^6 years timescale.

Most TAF models require a small but significant and persistent quadrupole (g_2^0) term, offsetting slightly the dipolar component of the field, to fit the global paleomagnetic dataset covering the last 5 Myr (Gubbins and Kelly, 1993; Hatakeyama and Kono, 2002; Johnson and Constable, 1995; McElhinny and McFadden, 1997; Quidelleur et al., 1994). However, some recent individual studies (e.g., Carlut et al., 2000; Yamamoto et al., 2002) from near equatorial sites, where such quadrupole effect should be best recorded, revealed inclination close to the GAD value, rendering the g_2^0 component unnecessary. Alternatively, a persistent g_2^0 component on the order of 5% of g_1^0 appears required to explain the mean direction recorded at other individual equatorial sites, such as in Indonesia (Elmaleh et al., 2004), for instance.

In the present study no persistent zonal term appears necessary to account for the small, not statistically significant at the 95% confidence level, departure form the axial dipole field. Furthermore, if any, the required g_2^0 component would be of negative sign of g_1^0, which is opposite of what observed in most global studies (Constable and Parker, 1988; Johnson and Constable, 1997; Merrill and McFadden, 2003; Quidelleur et al., 1994). Even when a persistent axial octupole g_3^0 is advocated (as sometimes proposed), it would be of opposite sign of what expected from these global studies. This suggests that no significant non-dipolar component could be derived from the present single study and that other data from South America should first be considered before deriving any regional mean paleomagnetic direction.

5.3 Comparison with previous results from the Americas and the southern hemisphere

Although South America was devoted of paleomagnetic data for TAF determinations when this study was initiated, a number of results have since been published. In southern Patagonia (Mejia et al., 2004), from 33 flows covering a time interval of 4 Myr, the mean direction (I=-68°; D=-1.3°; α_{95}=3.5°) is not statistically different from that of the GAD (expected inclination: -68°). Slightly to the north, another study in the Lago Buenos Aires area, yielded 26 directions covering the 0 to 3 Ma time interval (Brown et al., 2004). The mean direction (I=-63°; D=3.4°; α_{95}=5.4°) is also compatible with the GAD hypothesis (expected inclination: -62°). To the north of the present study, in Ecuador, Opdyke et al. (2006) reported a mean direction of (I=-5.4°; D=-0.1°; α_{95}=4.2°) for 51 flows younger than 2.6 Ma, which is only slightly different from the GAD, and is best modeled when a small (5% of g_1^0) axial quadrupole (g_2^0) is superimposed.

Within the central and northern Americas, three recent studies were conducted in Mexico, western US and Canada. While a g_2^0 term of 5% superimposed to the GAD is suggested in the former (Mejia et al., 2005) and the latter (Mejia et al., 2002), the GAD alone can account for the mean direction reported in the western US (Tauxe et al., 2004b). In addition, The GAD alone can also account for results obtained in many studies form a wide range of site location, such as Lesser Antilles (Carlut et al., 2000), French Polynesia (Yamamoto et al., 2002), Australia (Opdyke and Musgrave, 2004) and Antartica (Baraldo et al., 2003; Tauxe et al., 2004a).

5.4 Virtual geomagnetic poles

Virtual geomagnetic poles (VGP) calculated for each of the 31 final sites are reported in Table 1 and plotted in Figure 6. All VGP latitudes lie above 61°S (for reverse directions) and 59°N (for normal direction), which shows that no transitional direction was recorded here. This is not surprising, since when taking into account the total time interval covered here (about 1.3 Myr), the total number of transitions covered (4), the typical duration of a single transition (about 10 kyr maximum; e.g., Quidelleur et al., 2003), only 1 out of 130 flows would be statistically emitted during a polarity change. Even if excursions of the geomagnetic field are considered, although they occur quite often as observed within the Brunhes chron (Langereis et al., 1997), because of their probably shorter duration we would have statistically recorded one excursional direction at the most.

Figure 7 shows the scatter in paleomagnetic directions, represented by the angular dispersion of VGP (ASD) as a function of latitude for both the data from a global 0-5 Ma dataset (Quidelleur et al., 1994), and values derived from the C1 statistical model (Quidelleur and Courtillot, 1996). This model is close to the basic model of Constable and Parker (1988) as it assumes that each spherical harmonic coefficient vary as uniform random gaussian values with zero mean and decreasing standard deviation as a function of the degree. In order to improve the fit of the ASD increase with latitude observed for the data, the quadrupolar terms behave differently as a function of the spherical harmonic order. This shows that such simple model can accurately reproduce important observations concerning the paleomagnetic field properties. Note that the strength of the persistent axial quadrupole (g_2^0) has little influence regarding the increase of ASD with latitude (Constable and Parker, 1988). ASD values for the present study were calculated for normal and reverse directions (Table 4 and Figure 7). Normal data (closed star) are compatible with both the C1 model the global dataset while reverse data (open star) are significantly lower. All sites combined (grey star) are compatible with the model within uncertainty. When only data from the last 300 kyr are considered, the ASD is 16.7° (Table 4), in full agreement with the expected value for this site latitude (Figure 7). Note that similar conclusions are reached with model G of McFadden et al. (1988), and with other statistical field models (Constable and Johnson, 1999; Tauxe and Kent, 2004) that also fit well the global datasets.

It is interesting to compare our angular deviation values with other recent studies from nearby area. In southern Patagonia (Mejia et al., 2004), the VGP scatter of 17° is compatible with statistical PSV models (e.g., Quidelleur and Courtillot, 1996). In Ecuador, (Rochette et al., 1997) recorded an ASD of 11.2° in the Galapagos Islands during the 0-2 Ma interval, while on-land, (Opdyke et al., 2006) observed an ASD of 13.3° for the last

2.6 Myr, both results being also compatible with the expected value within uncertainties. On the other hand, a large scatter greater than 20° was obtained in the Lago Buenos Aires nearby area (Brown et al., 2004). Since many transitional directions (10 out of 36) have been reported there, we suspect that for unclear reasons this latter study is not representative of the PSV.

Regarding our PSV results for reverse directions (Table 4 and Figure 7) two hypotheses arise; either we do not have sampled enough the paleomagnetic secular variation during the 0.9 – 1.9 Ma time interval, or, the PSV was significantly lower during this interval. We think that the first hypothesis can be ruled out because of the relatively large geographic distribution of our sites within the LLVF (Figure 1), and because of the large time covered by these sites (Table 2a). However, only 12 sites display reverse directions, which might be insufficient for PSV investigations (Tauxe et al., 2003). Alternatively, the second hypothesis, if validated by other sites at this latitude, would have strong implications for our understanding of the timescales of the PSV. Finally, we note that in a recent compilation of new and previous data (Johnson et al., 2008) there is also, at this site latitude, a slight tendency (although not statistically significant) for a lower VGP dispersion during the reverse Matuyama chron (14.5°; N=40) than during the normal Brunhes chron (16.1°; N=194).

6. Conclusions

The mean direction (declination = 357.3°, inclination = -52.8°, α_{95} = 4.6°) from the 31 sites of the present study is compatible with the expected axial dipole field direction. Similar conclusions are reached when only normal or reverse directions are considered.

Other recent studies from South American sites (Brown et al., 2004; Mejia et al., 2004; Opdyke et al., 2006) also support a TAF without any non-zonal persistent components. On the other hand, they display slightly contradictory conclusions regarding the presence of a significant persistent zonal quadrupole term. It is not observed in southern Patagonia (Brown et al., 2004; Mejia et al., 2004), while a small positive term seems required in Ecuador (Opdyke et al., 2006). When considered together with our results, which show a slight tendency (although not statistically significant) for a small negative term, all presently available data from South America support an axial dipole only TAF.

PSV from normal and reverse polarity data display contrasting features. For normal directions, PSV is as expected for this site latitude, while VGP displays a very small dispersion for reverse data, all of them being from the 1.9 – 0.9 Ma time interval.

Finally, our results from South America increase the available number of recent high quality data from this area of the globe in particular, and from southern hemisphere sites in general. Together with their associated age constrains, they improve global datasets which will allow the construction of the next generation of TAF model which, hopefully, will allow the investigation of the 10^5 yr timescale variations.

Acknowledgements

We thank Diego Winocur for his help during sampling. Reviews by two anonymous referees were much appreciated. Funding was obtained from INSU CNRS DyETI program. This is LGMT contribution number 74.

References

Baraldo, A., Rapalini, A.E., Bohnel, H. and Mena, M., 2003. Paleomagnetic study of Deception Island, South Shetland Islands, Antarctica. Geophys. J. Int., 153: 333-343.

Bermudez, A., Delpino, D., Frey, F. and Saal, A., 1993. Los Basaltos de retroarco extraandinos. In: V.A.Ramos (Editor), XII° Congreso Geologico Argentino y II° Congreso de Exploracion de Hidrocarburos. Geologia y Recursos Naturales de Mendoza, Mendoza, pp. 161-172.

Brown, L.L., Singer, B.S. and Gorring, M.L., 2004. Paleomagnetism and Ar-40/Ar-39 chronology of lavas from Meseta del Lago Buenos Aires, Patagonia. Geochem. Geophys. Geosyst., 5.

Cande, S. and Kent, D., 1995. Revised calibration of the geomagnetic polarity time scale. J. Geophys. Res., 100: 6093-6095.

Carlut, J. and Courtillot, V., 1998. How complex is the time-averaged geomagnetic field over the past 5 million years? Geophys. J. Int., 134: 527-544.

Carlut, J., Quidelleur, X., Courtillot, V. and Boudon, G., 2000. Paleomagnetic directions and K/Ar dating of 0 to 1 Ma lava flows from La Guadeloupe Island (French West Indies): Inplications for time-averaged field models. J. Geophys. Res., 105: 835-849.

Cassignol, C. and Gillot, P.-Y., 1982. Range and effectiveness of unspiked potassium-argon dating: Experimental groundwork and applications. Numerical Dating in Stratigraphy. John Wiley, New York, 159-179 pp.

Cogné, J.P., 2003. Paleomac: a Macintosh application for treating paleomagnetic data and making plate reconstructions. Geochem. Geophys. Geosyst., 4(1): 1007.

Constable, C.G. and Johnson, C.L., 1999. Anisotropic paleosecular variation models: implications for geomagnetic observables. Phys. Earth Planet. Int., 115: 35-51.

Constable, C.G. and Parker, R.L., 1988. Statistics of the geomagnetic secular variation for the past 5 Myr. J. Geophys. Res., 93: 11569-81.

Cox, A., 1969. Confidence limits for the precision parameter k. Geophys. J. Roy. astr. Soc., 18: 545-549.

Elmaleh, A., Valet, J.P., Quidelleur, X., Solihin, A., Bouquerel, H., Tesson, T., Mulyadi, E., Khokhlov, A. and Wirakusumah, A.D., 2004. Palaeosecular variation in Java and Bawean Islands (Indonesia) during the Brunhes chron. Geophys. J. Int., 157: 441-454.

Fisher, R.A., 1953. Dispersion on a sphere. Proc. R. Soc. Lond., A217: 295-305.

Folguera, A., Zapata, T. and Ramos, V.A., 2006. Late Cenezoic extension and the evolution of the Neuquén Andes. In: S.M.K.a.V.A. Ramos (Editor), Evolution of an Andean Margin: a tectonic and magmatic view from the Andes to the Neuquén Basin (35°-39°S lat). The Geological Society of America, pp. 267-285 / 359.

Germa, A., Quidelleur, X., Gillot, P.Y. and Tchilingurian, P., 2008. Evolution of the back-arc Pleistocene volcanic complex of Payun Matru (Argentina) and its geodynamic implication for magma genesis in a complex slab geometry setting. submitted.

Gillot, P.-Y. and Cornette, Y., 1986. The Cassignol technique for potassium-argon dating, precision and accuracy: examples from late Pleistocene to recent volcanics from southern Italy. Chem. Geol., 59: 205-222.

Gillot, P.Y., Cornette, Y., Max, N. and Floris, B., 1992. Two reference materials, trachytes MDO-G and ISH-G, for argon dating (K-Ar and $^{40}Ar/^{39}Ar$) of Pleistocene and Holocene rocks. Geostandards Newsletter, 16(1): 55-60.

Gubbins, D. and Kelly, P., 1993. Persistent patterns in the geomagnetic field over the past 2.5 Myr. Nature, 365: 829-832.

Halls, H.C., 1976. A least-squares method to find a remanence direction from converging remagnetization circles. Geophys. J.R. astr. Soc., 45: 297-304.

Hatakeyama, T. and Kono, M., 2002. Geomagnetic field model for the last 5 My: time-averaged field and secular variation. Phys. Earth Planet. Int., 133: 181-215.

Johnson, C.L. and Constable, C.G., 1995. The Time-Averaged Geomagnetic-Field as Recorded by Lava Flows over the Past 5 Million-Years. Geophys. J. Int., 122: 489-519.

Johnson, C.L. and Constable, C.G., 1997. The time-averaged geomagnetic field: global and regional biases for 0-5 Ma. Geophys. J. Int., 131: 643-666.

Johnson, C.L., Constable, C.G., Tauxe, L., Barendregt, R., Brown, L.L., Coe, R.S., Layer, P., Mejia, V., Opdyke, N.D., Singer, B.S., Staudigel, H. and Stone, D.B., 2008. Recent investigations of the 0-5 Ma geomagnetic field recorded by lava flows. Geochem. Geophys. Geosyst., 9.

Kay, S.M., Burns, W.M., Copeland, P. and Mancilla, O., 2006. Upper Cretaceous to Holocene magmatism and avidence for transient Miocene shallowing of the Andean subduction zone under the northern Neuquén Basin. In: S.M.K.a.V.A. Ramos (Editor), Evolution of an Andean Margin: a tectonic and magmatic view from the Andes to the Neuquén Basin (35°-39°S lat). The Geological Society of America, pp. 19-60 / 359.

Kay, S.M., Gorring, M.L. and Ramos, V.A., 2004. Magmatic sources, setting and causes of Eocene to Recent Patagonian plateau magmatism (36°S to 52°S latitude). Rev. Asoc. Geol. Arg., 59: 556-568.

Khokhlov, A., Hulot, G. and Bouligand, C., 2006. Testing statistical palaeomagnetic field models against directional data affected by measurement errors. Geophys. J. Int., 167: 635-648.

Khokhlov, A., Hulot, G. and Carlut, J., 2001. Towards a self-consistent approach to palaeomagnetic field modelling. Geophys. J. Int., 145: 157-171.

Kirschvink, J., 1980. The least-squares line and plane and the analysis of paleomagnetic data: examples from Siberia and Morocco. Geoph. J. Royal Astr. Soc., 62: 699-718.

Kono, M. and Tanaka, H., 1995. Mapping the Gauss coefficients to the pole and the models of paleosecular variation. J. Geomagn. Geoelec., 47: 115-130.

Langereis, C.G., Dekkers, M.J., de Lange, G.J., Paterne, M. and van Santvoort, P.J.M., 1997. Magnetostratigraphy and astronomical calibration of the last 1.1 Myr from an eastern Mediterranean piston core and dating of short events in the Brunhes. Geophys. J. Int., 129: 75-94.

Lawrence, K.P., Constable, C.G. and Johnson, C.L., 2006. Paleosecular variation and the average geomagnetic field at ±20° latitude. Geochem. Geophys. Geosyst., 7.

McElhinny, M. and McFadden, P., 1997. Palaeosecular variation over the past 5 Myr based on a new generalized database. Geophys. J. Int., 131: 240-252.

McFadden, P.L., Merrill, R.T. and McElhinny, M.W., 1988. Dipole/quadrupole family modeling of paleosecular variation. J. Geophys. Res., 93: 11,583-11,588.

Mejia, V., Barendregt, R.W. and Opdyke, N.D., 2002. Paleosecular variation of Brunhes age lava flows from British Columbia, Canada. Geochem. Geophys. Geosyst., 3.

Mejia, V., Bohnel, H., Opdyke, N.D., Ortega-Rivera, M.A., Lee, J.K.W. and Aranda-Gomez, J.J., 2005. Paleosecular variation and time-averaged field recorded in late Pliocene-Holocene lava flows from Mexico. Geochem. Geophys. Geosyst., 6.

Mejia, V., Opdyke, N.D., Vilas, J.F., Singer, B.S. and Stoner, J.S., 2004. Plio-Pleistocene time-averaged field in southern Patagonia recorded in lava flows. Geochem. Geophys. Geosyst., 5.

Merrill, R.T. and McFadden, P.L., 2003. The geomagnetic axial dipole field assumption. Phys. Earth Planet. Inter., 139: 171-185.

Odin, G.S. and 35 others, 1982. Interlaboratory standards for dating purposes. In: G.S. Odin (Editor), Numerical dating in stratigraphy. John Wiley and Sons, Chichester, pp. 123-150.

Opdyke, N.D., Hall, M., Mejia, V., Huang, K. and Foster, D.A., 2006. Time-averaged field at the equator: Results from Ecuador. Geochem. Geophys. Geosyst., 7.

Opdyke, N.D. and Musgrave, R., 2004. Paleomagnetic results from the Newer Volcanics of Victoria: Contribution to the time averaged field initiative. Geochem. Geophys. Geosyst., 5.

Pasquaré, G., Bistacchi, A., Francalanci, L., Bertotto, G.W., Boari, E., Massironi, M. and Rossotti, A., 2008. Very long Pahoehoe inflated basaltic lava flows in the Payenia volcanic province (Mendoza and La Pampa, Argentina). Rev. Asoc. Geol. Arg., 63: 131-149.

Quidelleur, X., Carlut, J., Soler, V., Valet, J.-P. and Gillot, P.-Y., 2003. The age and duration of the Matuyama-Brunhes transition from new K-Ar data from La Palma (Canary Islands) and revisited $^{40}Ar/^{39}Ar$ ages. Earth Planet. Sci. Lett., 208: 149-163.

Quidelleur, X. and Courtillot, V., 1996. On low-degree spherical harmonic models of paleosecular variation. Phys. Earth Planet. Inter., 95: 55-77.

Quidelleur, X., Gillot, P.Y., Soler, V. and Lefèvre, J.C., 2001. K/Ar dating extended into the last millennium:

Application to the the youngest effusive episode of the Teide volcano (Spain). Geophys. Res. Lett., 28: 3067-3070.

Quidelleur, X., Valet, J.P., Courtillot, V. and Hulot, G., 1994. Long-term geometry of the geomagnetic field for the last five million years: An updated secular variation database. Geophys. Res. Letters, 21: 1639-42.

Ramos, V.A., 1999. Plate tectonic setting of the Andean Cordillera. Episodes, 22: 183-190.

Ramos, V.A. and Kay, S.M., 2006. Overview of the tectonic evolution of the southern Central Andes of Mendoza and Neuquén (35°-39° latitude). In: S.M.K.a.V.A. Ramos (Editor), Evolution of an Andean Margin: a tectonic and magmatic view from the Andes to the Neuquén Basin (35°-39°S lat). The Geological Society of America, pp. 1-17 / 359.

Rochette, P., Ben Atig, F., Collombat, H., Vandamme, D. and Vlag, P., 1997. Low paleosecular variation at the equator: a paleomagnetic pilgrimage from Galapagos to Esterel with Allan Cox and Hans Zijderveld. Geologie En Mijnbouw, 76(1-2): 9-19.

Schneider, D.A. and Kent, D.V., 1990. The time-averaged paleomagnetic field. Rev. Geophys., 28: 71-96.

Tauxe, L., 2005. Inclination flattening and the geocentric axial dipole hypothesis. Earth Planet. Sci. Lett., 233: 247-261.

Tauxe, L., Constable, C., Johnson, C.L., Koppers, A.A.P., Miller, W.R. and Staudigel, H., 2003. Paleomagnetism of the southwestern USA recorded by 0-5 Ma igneous rocks. Geochem. Geophys. Geosyst., 4.

Tauxe, L., Gans, P. and Mankinen, E.A., 2004a. Paleomagnetism and Ar-40/Ar-39 ages from volcanics extruded during the Matuyama and Brunhes Chrons near McMurdo Sound, Antarctica. Geochem. Geophys. Geosyst., 5.

Tauxe, L. and Kent, D.V., 2004. A simplified statistical model for the geomagnetic field and the detection of shallow bias in paleomagnetic inclinations: Was the ancient magnetic field dipolar?, Timescales of the Paleomagnetic Field. Geophysical Monograph Series. A. G. U., Washington, pp. 101-115.

Tauxe, L., Luskin, C., Selkin, P., Gans, P. and Calvert, A., 2004b. Paleomagnetic results from the Snake River Plain: Contribution to the time-averaged field global database. Geochem. Geophys. Geosyst., 5.

Wilson, R., 1971. Dipole offset - the time-averaged palaeomagnetic field over the past 25 Ma. Geophys. J. Roy. Astr. Soc., 22: 491-504.

Yamamoto, Y., Shimura, K., Tsunakawa, H., Kogiso, T., Uto, K., Barsczus, H.G., Oda, H., Yamazaki, T. and

Kikawa, E., 2002. Geomagnetic paleosecular variation for the past 5 Ma in the Society Islands, French Polynesia. Earth Planets Space, 54: 797-802.

Zanella, E., 1998. Paleomagnetism of Pleistocene volcanic rocks from Pantelleria Island (Sicily channel) Italy. Phys. Earth Planet. Int., 108: 291-303.

Zijderveld, J.D.A., 1967. A.C. demagnetization of rocks: Analysis of results. In: D.W. Collinson, K.M. Creer and S.K. Runcorn (Editors), Methods in paleomagnetism. Elsevier, New York, pp. 254-286.

Figure captions

Figure 1: Location of sampled areas. K/Ar ages previously available for PMVF (Germa et al., 2008) and obtained herein are given in ka.

Figure 2: Typical demagnetization diagrams. Zijderveld projections obtained during thermal and AF demagnetization for reverse (a) and normal polarity flows (b). Zijderveld and stereographic projections of a reverse (resp. normal) sample affected by a slight IRM easily removed during AF (c; resp. e), but not during thermal treatment (d; resp. f). In zijderveld projections, solid symbols correspond to projections onto the horizontal plane, while open symbols are projections onto the vertical plane. For stereographic projections, solid and open symbols indicate directions in the upper and lower hemisphere, respectively.

Figure 3: Stereographic projection of individual flow directions. Rejected flow directions (see text) are labeled and shown in grey.

Figure 4: Stereographic projections a) all remaining normal and reverse polarity flows (N=31), b) flows from the 1.9 – 0.9 Ma time interval (N=13) and c) flows from the last 300 kyr (N=18). Same symbols as in Figure 3. The open star in b) and c) shows the mean direction.

Figure 5: Comparison between the magnetic polarity of dated flows from this study with the geomagnetic polarity time scale (Cande and Kent, 1995). Closed and open symbols are for flows with normal and reverse polarity, respectively. All ages are in Ma. Note that for PN and PY flows the age uncertainty is lower than the symbol size.

Figure 6: VGP positions shown with their α_{95} confidence interval for a) all flows, b) normal polarity flows and c) reverse polarity flows.

Figure 7: VGP scatter in terms of the ASD obtained from this study (star) plotted as a function of latitude and compared with values of C1 model (black curve) and values derived from their global dataset (grey curve)

(Quidelleur and Courtillot, 1996). Close, white and grey stars are for normal, reverse and both polarity data, respectively (see Table 4). Uncertainties were obtained from Cox (1969).

Table captions

Table 1: Paleomagnetic directions. Column headings indicate Site # , flow location: Lat. (site latitude), Long. (Site longitude), n/N (number of data used/total number of samples measured), Dec. (declination, in degree), Inc. (inclination, in degree), α_{95} (radius of the 95% confidence cone from *Fisher* (Fisher, 1953) statistics), λ (virtual geomagnetic pole latitude), ϕ (virtual geomagnetic pole longitude), Comment (N GtC = N great circle analyses were used).

Table 2: New Cassignol-Gillot K-Ar ages from a) the Cero Nevado volcanic field, and b) the Payun Matru Volcanic field ($^{40}Ar^{*}$ (%): radiogenic argon 40 in percent; $^{40}Ar^{*}$ (x10^{12} at/g): radiogenic argon 40 in number of atoms per gram of sample).

Table 3: Previous K-Ar ages from the Payun Matru volcanic field (Germa et al., 2008).

Table 4: Mean directions paleomagnetic results. n (number of average directions), Dec (mean declination, in degree), Inc (mean inclination, in degree), k (kappa precision parameter), α_{95} (radius of the 95% confidence cone from *Fisher* (Fisher, 1953) statistics), ΔI (observed inclination – dipole inclination, in degree), VGP lat. (virtual geomagnetic pole latitude), VGP long. (virtual geomagnetic pole longitude), ASD (angular standard deviation) , VGP sc. (VGP scatter around the mean VGP pole).

Table 1.

Site	Lat.	Long.	n/N	Dec (°)	Inc (°)	k	α_{95}	VGP lat.	VGP long.	Comment
CN01	-35.51942	-68.64081	8/9	216.1	-61.5	256.4	3.5	-61.3	-133.1	
CN02	-35.50167	-68.62328	6/9	190.4	-53.8	140.2	5.8	-81.4	196.7	2 GtC
CN05	-35.63069	-68.53278	10/10	173.4	-57.3	248.8	3.1	-84.2	-4.1	
CN07	-35.58919	-68.50011	7/7	179.8	-60.0	391.8	3.1	-84.7	-66.9	
CN08*	-35.59308	-68.50361	6/8	171.7	-55.8	383.2	3.6	-	-	2 GtC
CN09*	-35.62939	-68.53036	7/9	168.4	-54.4	108.4	5.8	-	-	
CN10	-35.62939	-68.53036	7/8	177.8	-56.5	232.6	4.0	-87.7	-18.8	
CN11	-35.59939	-68.63992	7/8	344.4	-51.2	256.4	4.0	76.5	-147.0	3 GtC
CN33	-35.76556	-68.29103	9/9	178.8	-39.6	48.1	7.7	-76.6	106.9	3 GtC
CN34	-35.77406	-68.29867	4/7	10.8	-60.8	39.9	15.6	-	-	1 GtC
CN36	-35.32572	-68.38858	9/9	180.7	-47.8	39.5	8.3	-83.5	117.1	
CN37*	-35.32572	-68.38858	8/9	179.6	-31.2	25.0	11.6	-	-	3 GtC
CN38*	-35.32833	-68.36644	5/8	180.8	-34.6	573.2	3.2	-	-	
CN39	-35.28722	-68.23881	3/4	154.6	-34.4	63.6	15.6	-	-	
CN40*	-35.25014	-68.25347	8/9	179.7	-53.6	41.1	8.7	-	-	
CN42*	-35.21561	-68.25564	6/8	181.5	-50.4	192.1	4.8	-	-	
CN44	-35.18006	-68.24900	8/9	178.7	-45.6	48.1	8.2	-81.8	103.7	2 GtC
PN15	-36.42375	-69.66111	8/9	0.6	-47.3	101.4	5.5	82.0	-65.9	
PN16	-36.42389	-69.66008	6/8	4.6	-62.3	149.7	5.5	82.0	85.7	
PN17	-36.31331	-69.66397	7/7	347.7	-51.7	260.1	3.7	79.1	-142.0	
PN22	-36.39422	-69.39839	6/6	343.1	-42.3	221.0	4.5	71.2	-124.7	
PN23	-36.44211	-69.38072	7/7	331.4	-36.9	95.8	6.2	60.5	-134.8	
PN24	-36.48217	-69.37269	5/8	8.1	-50.9	391.7	3.9	81.7	-13.2	
PN25	-36.48217	-69.37269	5/8	348.7	-65.7	56.9	10.2	75.9	143.2	
PN26	-36.51331	-69.34542	6/8	354.2	-62.5	1398.5	1.8	81.4	140.0	
PY12	-36.43792	-69.63217	8/9	12.7	-62.0	96.0	5.7	78.1	59.4	1 GtC
PY14	-36.47342	-69.64694	8/8	2.5	-55.8	158.3	4.4	88.0	16.7	
PY15*	-36.53731	-69.61611	6/8	17.2	-64.3	226.2	4.5	-	-	
PY16*	-36.53800	-69.61839	7/7	16.1	-63.6	384.0	3.1	-	-	
PY18	-36.47228	-69.37975	6/8	328.5	-61.5	16.2	17.2	-	-	
PY19	-36.47311	-69.38047	6/8	3.1	-54.6	245.5	4.3	87.1	-7.1	
PY20	-36.37281	-69.40289	5/7	350.2	-64.3	94.8	7.9	77.8	144.7	
PY21*	-36.21300	-69.39747	7/7	165.4	59.8	86.7	6.5	-	-	
PY22*	-36.18450	-69.40069	5/5	170.5	58.6	180.0	6.1	-	-	2 GtC
PY26	-36.30239	-69.33172	7/7	352.1	-59.8	74.8	7.2	82.4	163.1	2 GtC
PY27	-36.30953	-69.29875	8/10	344.8	-29.3	65.6	6.9	65.3	-106.5	
PY28	-36.30794	-69.29669	5/9	4.2	-49.5	4869.5	1.2	83.1	-37.6	2 GtC
PY29	-36.37392	-69.21347	7/8	330.3	-69.0	178.5	4.7	63.7	153.7	3 GtC
PY31	-36.38031	-69.21014	5/7	27.3	-55.3	41.1	15.0	-	-	4 GtC
PY32	-36.39375	-69.21911	7/7	6.9	-12.2	113.9	5.9	59.1	-55.7	3 GtC
CN08-09	-	-	14/17	172.2	56.0	84.8	4.4	-83.6	10.7	
CN37-38	-	-	11/13	182.9	33.1	163.0	3.6	-72.6	120.8	
CN40-42	-	-	14/14	180.5	52.2	64.3	5.0	-87.6	121.7	
PY15-16	-	-	13/13	16.6	-63.9	315.1	2.3	74.6	61.6	
PY21-22	-	-	11/12	166.0	58.0	219.2	3.1	-78.6	3.9	

Table 2a.

Flow	K (%)	^{40}Ar* (%)	^{40}Ar* (x10^{12}at/g)	Age ± 1σ (Ma)	Mean (Ma)	Sample
CN03	1.742	26.2%	1.9020	1.045 ± 0.015		
		32.9%	1.8973	1.043 ± 0.015	1.044 ± 0.015	94D2
CN07	2.246	44.1%	3.1038	1.323 ± 0.019		
		47.1%	3.1210	1.330 ± 0.019		
		46.8%	3.0954	1.319 ± 0.019	1.324 ± 0.019	94I
CN10	3.398	29.7%	4.6662	1.314 ± 0.019		
		31.3%	4.7066	1.326 ± 0.019	1.320 ± 0.019	94L
CN11	0.790	16.9%	0.83289	1.009 ± 0.015		
		21.2%	0.85197	1.032 ± 0.015	1.022 ± 0.015	94M
CN34	0.914	28.0%	1.7882	1.872 ± 0.027		
		21.9%	1.7999	1.884 ± 0.028	1.878 ± 0.028	94BB
CN36	0.794	24.3%	1.1148	1.344 ± 0.020		
		10.4%	1.1380	1.372 ± 0.020	1.352 ± 0.020	94BD
CN42	0.882	16.0%	0.86756	0.942 ± 0.015		
		5.5%	0.87565	0.950 ± 0.022	0.944 ± 0.016	94BJ

Table 2b.

Flow	K (%)	^{40}Ar* (%)	^{40}Ar* (x10^{12}at/g)	Age ± 1σ (Ma)	Mean (Ma)	Sample
PY21	0.811	28.1	1.4547	1.717 ± 0.025		
		29.1	1.4543	1.716 ± 0.025	1.716 ± 0.025	94X

Table 3.

Flow	Age ± 1 σ (κα)	Sample
PN16	233 ± 11	88R
PN17	26 ± 5	88S
PN23	26 ± 2	88Z
PN25	9 ± 6	88AB
PN26	285 ± 5	88AC
PY27	15 ± 1	94AE
PY28	28 ± 5	94AF
PY29	168 ± 4	94AH1
PY31	82 ± 2	94AK
PY32	7 ± 1	94AL

Table 4.

Data	n	Dec (°)	Inc (°)	k	α_{95}	ΔI (°)	VGP lat.	VGP long.	ASD	VGP sc.
All	31	357.3	-52.8	32.6	4.6	2.7	87.5	233.9	14.8	14.6
N polarity	19	354.8	-53.0	25.6	6.8	2.5	85.8	214.9	16.5	15.9
R polarity	12	181.0	52.3	54.2	5.9	-3.2	-87.9	137.7	12.5	12.3
< 300 ka	18	355.5	-53.1	24.4	7.1	2.4	86.4	215.4	16.7	16.2
0.9 – 1.9 Ma	13	359.7	-52.3	55.2	5.6	3.2	88.0	-73.7	12.6	12.5

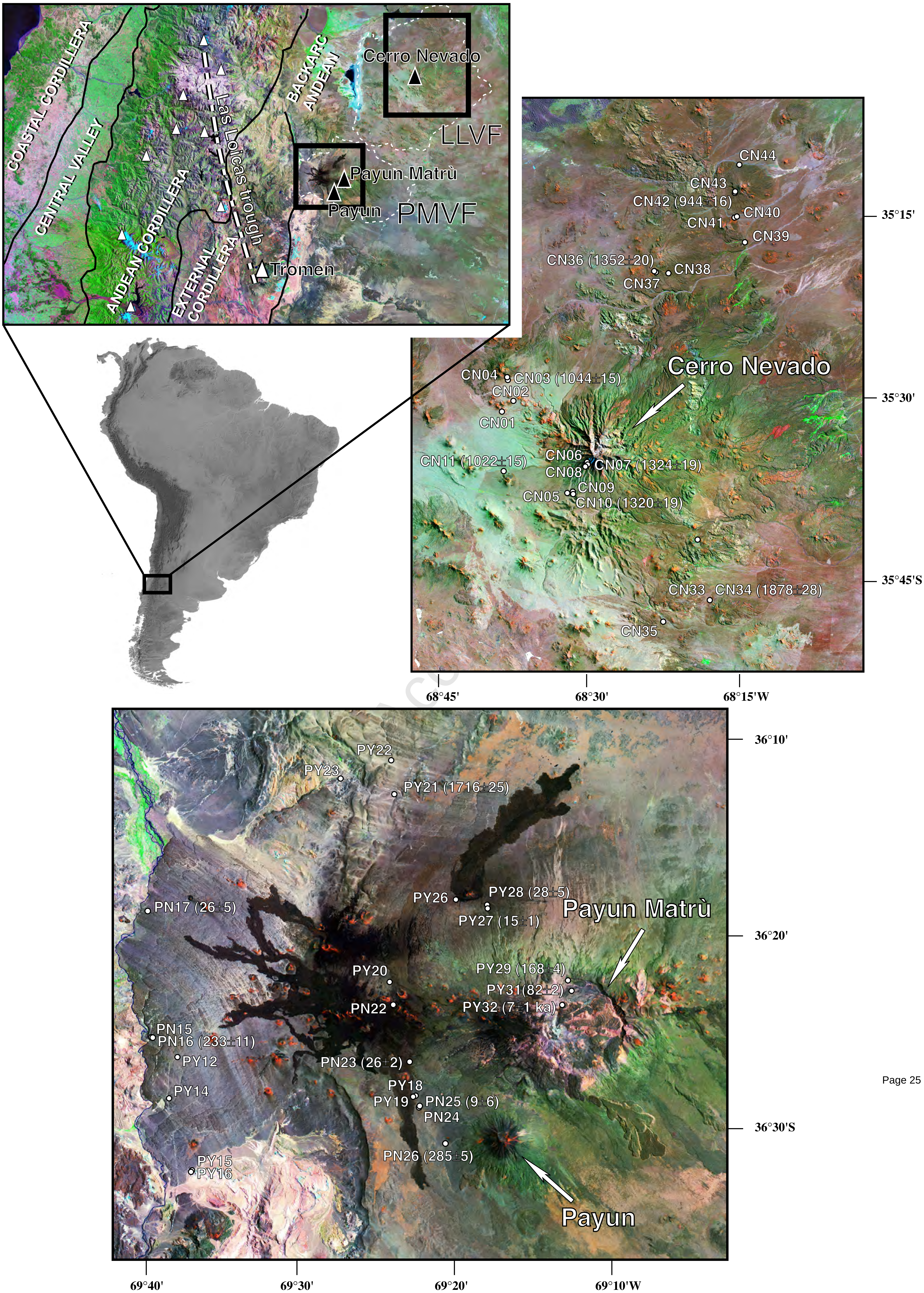

Figure 1 (Quidelleur et al., 2008)

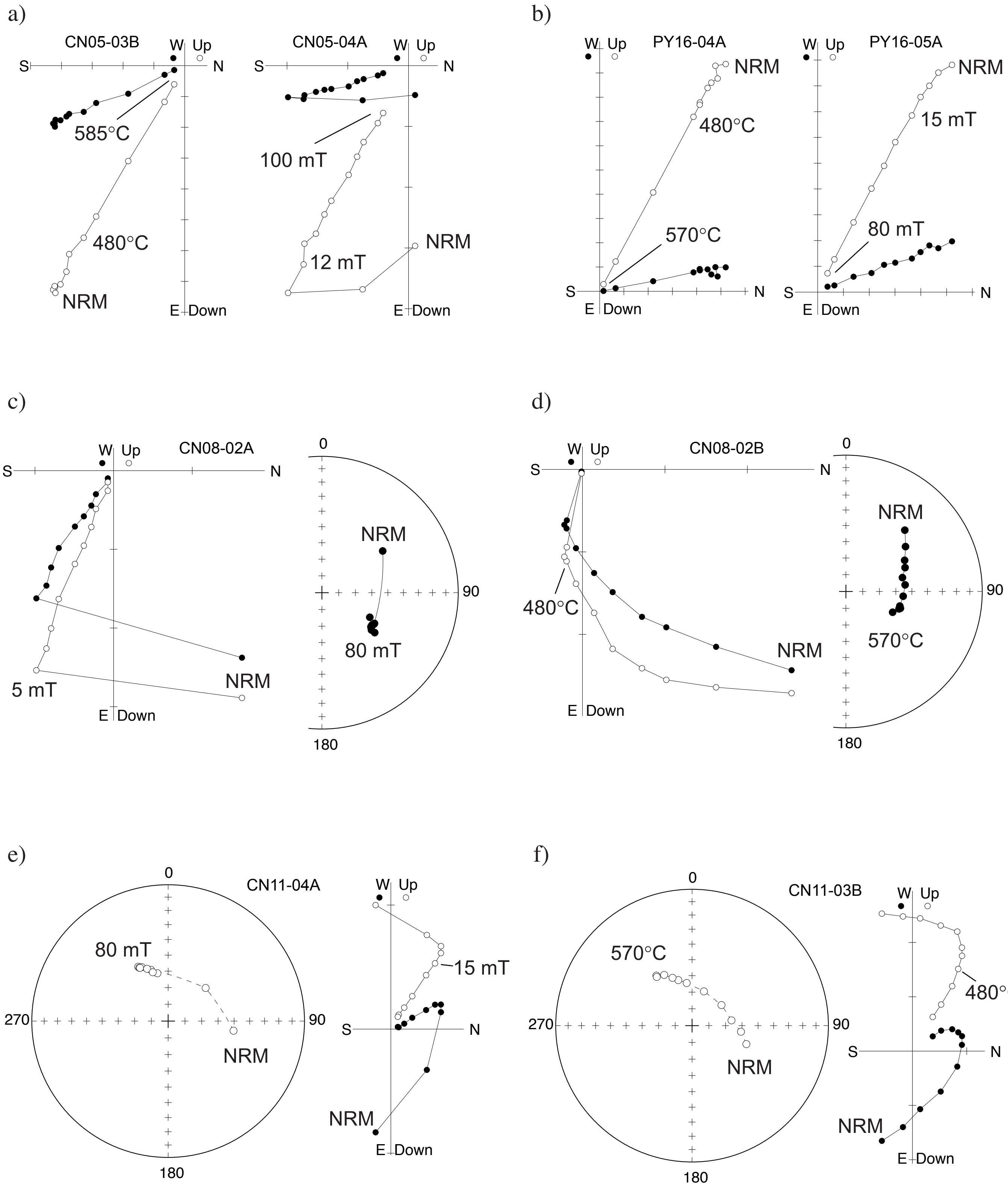

Figure 2 (Quidelleur et al., 2008)

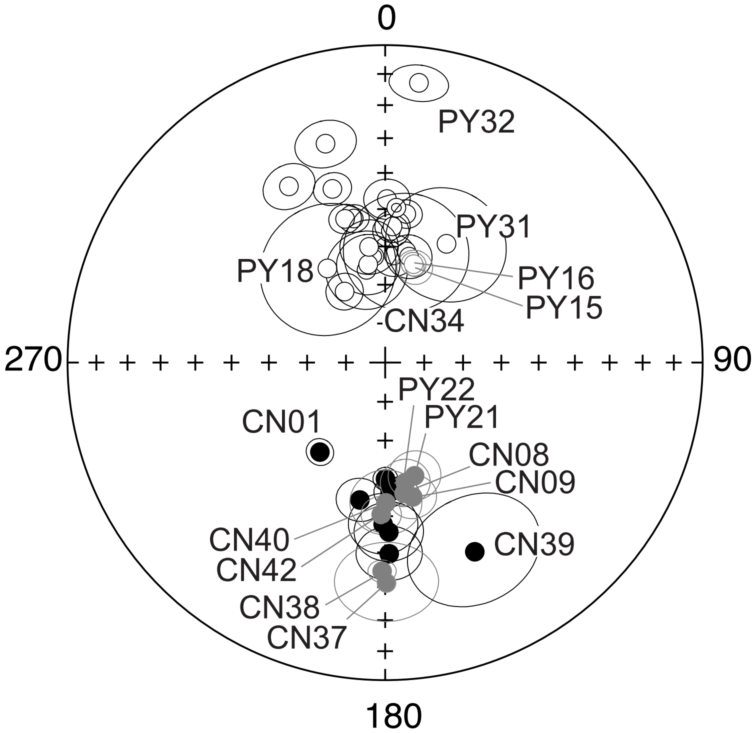

Figure 3 (Quidelleur et al., 2008)

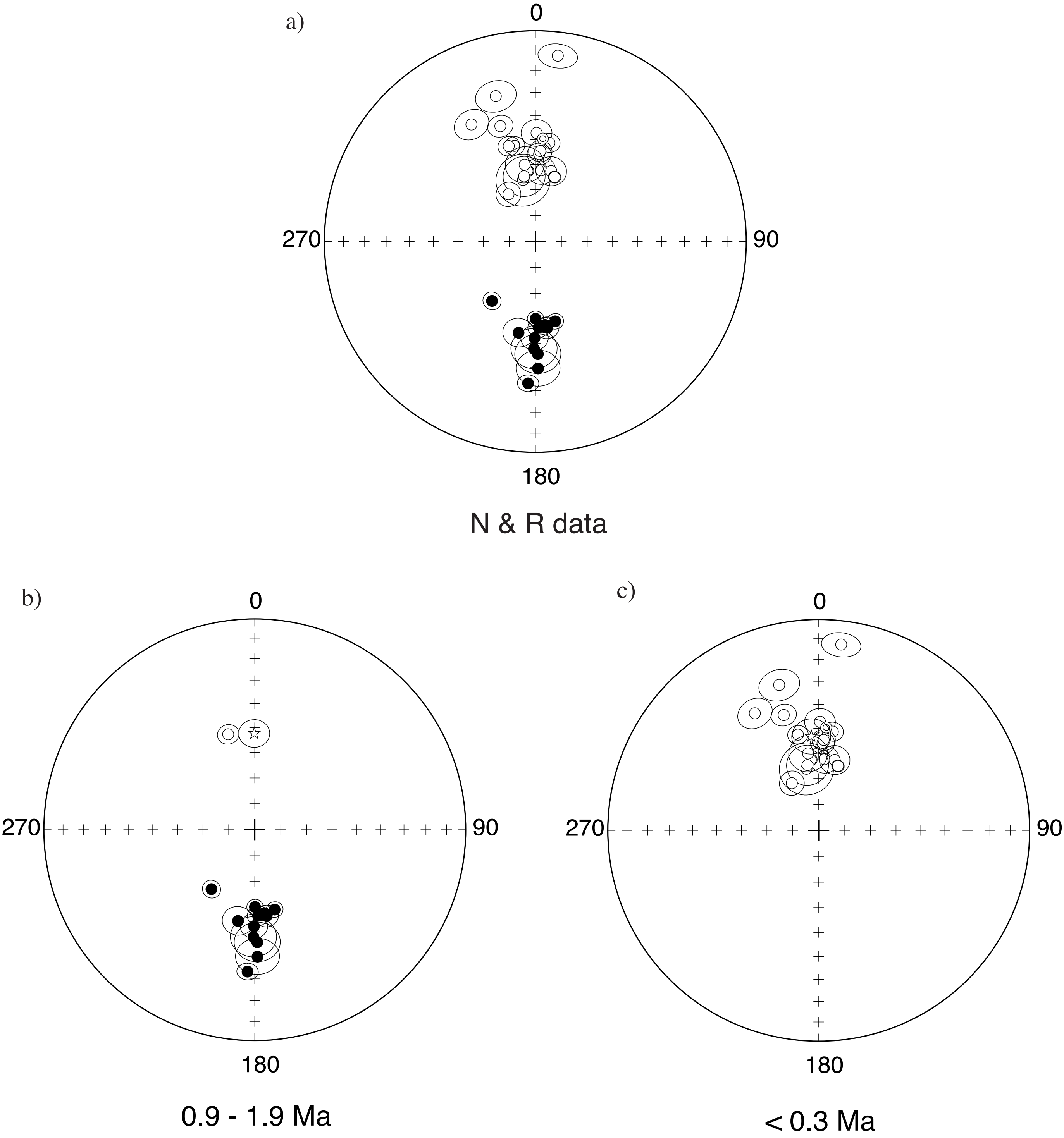

Figure 4 (Quidelleur et al., 2008)

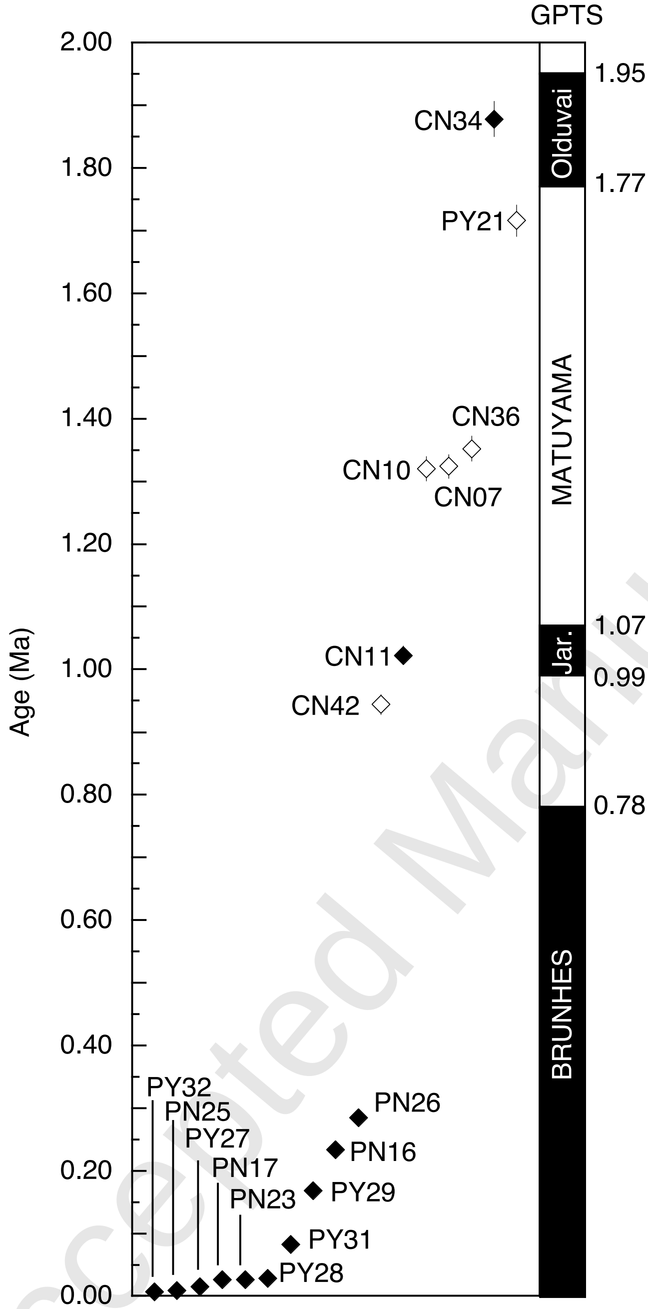

Figure 5 (Quidelleur et al., 2008)

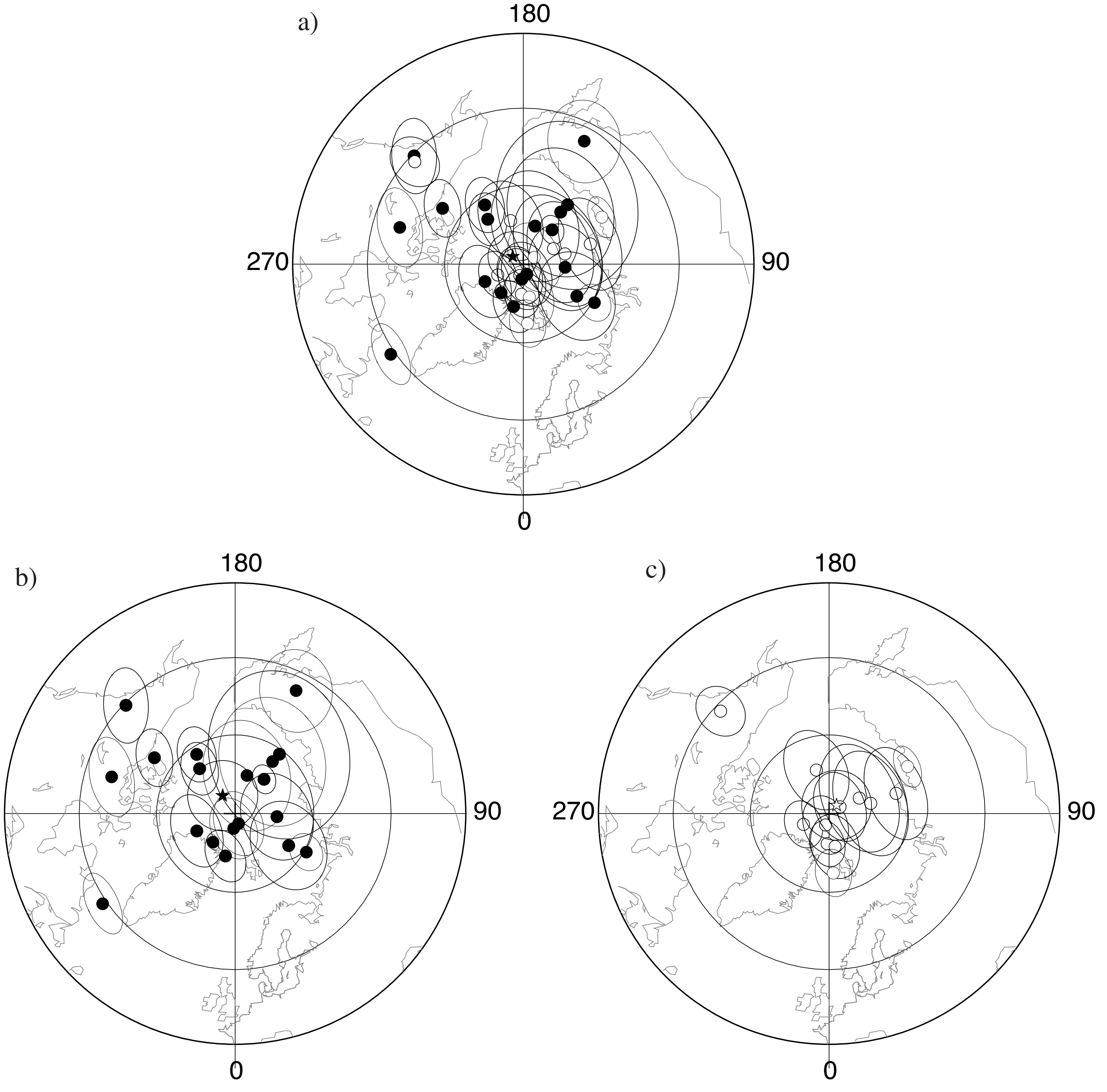

Figure 6 (Quidelleur et al., 2008)

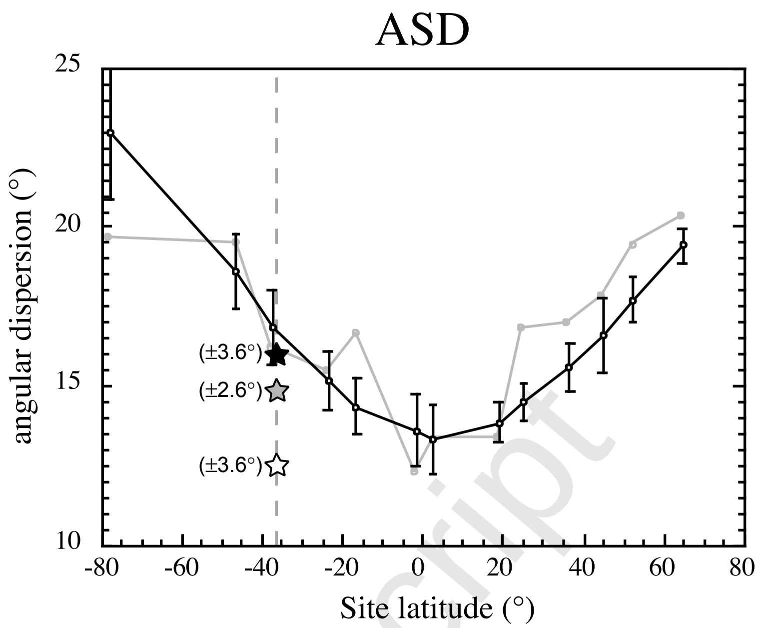

Figure 7 (Quidelleur et al., 2008)